NUMERICAL INVESTIGATION OF THE INDEX OF THE VECTOR FIELD OF HOLLING-TANNER MODEL BY THE FAST FOURIER TRANSFORM

A.A. ADENIJI*, I. FEDOTOV, M.Y. SHATALOV, A.C. MKOLESIA

Department of Mathematics, and Statistics, Tshwane University of Technology, Pretoria, South Africa

Abstract. The following Van der Pol and Holling-Tanner equations is analyzed from the qualitative viewpoint by investigating their vector fields and analyzing the nature of the stationary points of these equations. The winding numbers (indices) of the stationary points are investigated by calculating the Poincare integrals. This calculation is performed by a novel method which is based on application of the fast Fourier transform (FFT) formation to the Poincare integrand.

Keywords: Holling-Tanner; vector field; fast Fourier transform; index/winding number; stationary point; inverse problem.

2010 AMS Subject Classification: 65L09, 65L15, 65T60, 65T40, 65P40.

1. INTRODUCTION

The vector field represents vectors with components $X = X(x,y)$ and $Y = Y(x,y)$ in Oxy rectangular coordinated system, where X and Y are right hand sides/parts of the system of equations:

$$(1) \qquad \begin{cases} \dfrac{dx}{dt} = X(x,y), \\ \dfrac{dy}{dt} = Y(x,y). \end{cases}$$

*Corresponding author

E-mail address: adejimi.adeniji@gmail.com

Stationary points of this system are calculated as solution of the system of equation

$$
(2) \qquad \begin{cases} X(x,y) = 0, \\ Y(x,y) = 0. \end{cases}
$$

Index (winding number) of the stationary points is calculated by the Poincare integral:

$$
(3) \qquad I = \frac{1}{2\pi} \cdot \int_{AB} \frac{X(x,y) \cdot Y'(x,y) - X'(x,y) \cdot Y(x,y)}{X^2(x,y) + Y^2(x,y)} dp,
$$

where dp is a differential along the curve AB in Oxy-coordinate system, surrounding the stationary point, $x = x(p)$, and $y = y(p)$. According to [1], a Lipschitz continuous function of a plane vector field $\mathbf{F} = [X(x,y), Y(x,y)]$ over a smooth Jordan curve is considered over the integral (Poincare's integral).

It is obvious that integrand of the Poincare's integral

$$
(4) \qquad f(p) = \frac{\bar{X}(p) \cdot \bar{Y}'(p) - \bar{X}'(p) \cdot \bar{Y}(p)}{\bar{X}^2(p) + \bar{Y}^2(p)}.
$$

is 2π-periodic function, where

$$
(5) \qquad \bar{X}(p) = X(x(p), y(p)), \bar{Y}(p) = Y(x(p), y(p)).
$$

Due to 2π-periodicity of $f(p)$, we can expand it in the Fourier series

$$
(6) \qquad f(p) = \frac{a_0}{2} + \sum_{m=1}^{\infty} [a_m \cdot \cos(mp) + b_m \cdot \sin(mp)],
$$

where

$$
a_m = \frac{1}{\pi} \cdot \int_0^{2\pi} f(p) \cdot \cos(mp) dp,
$$

and

$$
(7) \qquad b_m = \frac{1}{\pi} \cdot \int_0^{2\pi} f(p) \cdot \sin(mp) dp.
$$

In these terms, the Poincare integral

$$
(8) \qquad f(p) = \frac{1}{2\pi} \cdot \int_0^{2\pi} f(p) dp = a_0,
$$

and can be found numerically by any discrete Fourier transformation (DFT). For example, the FFT, which is calculated from $N = 2^n$ (n is positive integer) samples of $f(p)$ which are equidistantly located at $p \in [0, 2\pi]$, i.e in $P_i = \frac{2\pi}{N} \cdot i, i = 0, 1, \ldots, N-1$. One of the advantages of FFT is

its speed which it gets by reducing the number of calculations needed to analyze waveform [2]. This is an alternative to DFT, because of the speed the algorithm reduces an n-points of Fourier transform to about $\frac{n}{2}log2(n)$. FFT is widely used in many applications in engineering, science, and mathematics such as speech processing and frequency estimation [3]. The fundamental idea of the algorithm was firstly derived in 1805 according to [4]. Recently the FFT algorithm was used to analyzed and detected the frequency with respect to the noise level using the white Gaussian noise [5]. The FFT algorithm (also known as Cooley-Turkey algorithm) was formulated by James W. Cooley and John W. Tukey in 1965 [6] and it is the most important numerical algorithm in applications.

Examples of FFT algorithm are ①Rader's FFT algorithm, ②Prime-factor FFT algorithm, ③Chirp Z-transform, ④Bruun's FFT algorithm, ⑤Bluestein's FFT algorithm, ⑥Hexagonal FFT, etc. It is of great importance to numerically investigate the dynamical systems (Van der pol and Holling-Tanner equation) considered in this study, through software MathCad® and Mathematica® for the vector plot, equilibrium points, and indices of the stationary points of the vector fields.

2. PROBLEM STATEMENT

This paper is devoted to the numerical analysis of the vector fields of the Van der Pol and Holling-Tanner systems by the built-in methods of the Mathematica® by means of numerical calculations of the indices of these fields by the FFT. The aims of the study were to:

- Obtain the equilibrium points of the Van der Pol and Holling-Tanner systems.
- Investigate the vector fields of the Van der Pol and Holling-Tanner systems by the built-in functions of Mathematica®.
- Calculate the indices of stationary points of the vector fields of the Van der Pol and Holling-Tanner models.

3. MODEL EXAMPLE: VECTOR FIELD AND INDEX OF THE STATIONARY POINT OF VAN DER POL EQUATION

In this section, we consider the well known Van der Pol equation and illustrate our approach to calculate the index of the stationary point of the vector field of this equation.

Let us represent Van der Pol equation

(9) $$\ddot{x} - (1 - x^2)\dot{x} + x = 0,$$

in the Cauchy form as

(10) $$\begin{cases} \dot{x} = y = X(x,y), \\ \dot{y} = (1 - x^2) \cdot y - x = Y(x,y). \end{cases}$$

The unique stationary point of this equation is

(11) $$x = 0, \quad y = 0.$$

Let us draw the vector field of this equation using the built-in function of the Mathematica® software. We plot the vector field of the Van der Pol by *ListStreamPlot* built-in function of the Mathematica® in the $x \in [-4,4], y \in [-4,4]$.
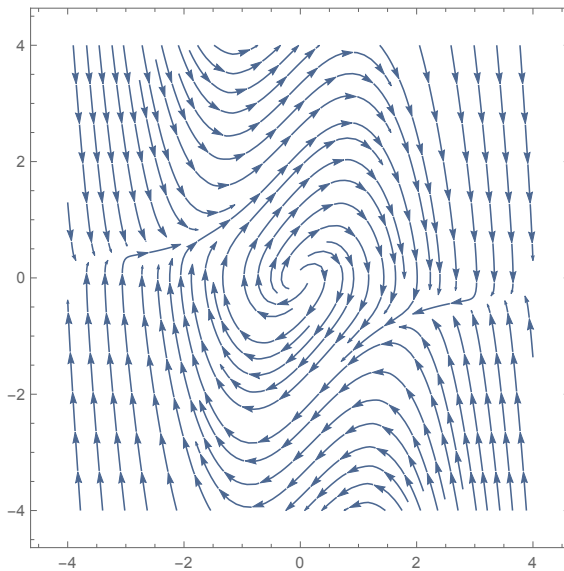
Figure (1) illustrates the obtained vector field.

Figure 1. *Vector field of Van-Der-Pol equation*

Linearization of Equation (10) in vicinity of $x = 0, \quad y = 0$ gives us the system

(12) $$\begin{cases} \dot{x} \cong y, \\ \dot{y} \cong -x + y, \end{cases}$$

and hence, the characterization equation is

$$\det \begin{bmatrix} -\lambda & 1 \\ -1 & 1-\lambda \end{bmatrix} = (\lambda)^2 - (\lambda) + 1 = 0.$$

from which it follows that the eigenvalues are

$$(13) \qquad \qquad \lambda_{1,2} = \frac{1 \pm i\sqrt{3}}{2} \cong 0.5 \pm i0.8660,$$

where i is complex unit ($i^2 = -1$).

Hence, the stationary point $x = y = 0$ is unstable focus (source). In the case of sources and sinks, the index of the stationary points is equal to $+1$ and in the core of the sinks, its equal to -1. To calculate the index numerically, we assume

$$(14) \qquad \qquad x = \rho \cdot \cos\theta; y = \rho \cdot \sin\theta, \text{where } \rho \text{ is constant}$$

hence

$$(15) \qquad \qquad X(\theta) = \rho \cdot \sin\theta, \ \ Y(\theta) = (1 - \rho^2\cos^2\theta)\rho \cdot \sin\theta - \rho\cos\theta,$$

and

$$(16) \qquad \qquad f(\theta) = \frac{Y(\theta) \cdot \frac{dX(\theta)}{d\theta} - \frac{dY(\theta)}{d\theta} \cdot X(\theta)}{X^2(\theta) + Y^2(\theta)}.$$

Let $\psi(\theta)$ and $\kappa(\theta)$ be represented in Equation (17)

$$
\begin{aligned}
(17) \qquad \psi(\theta) &= 1 + \rho^2 \cdot (\frac{1}{2}\sin 2\theta - \frac{1}{4}\sin 4\theta), \\
\kappa(\theta) &= -\frac{3}{2} + \sin 2\theta + \frac{1}{2}\cos 2\theta + \rho^2 \cdot (\frac{1}{4} - \frac{1}{2}\sin 2\theta - \frac{1}{4}\sin 4\theta - \frac{1}{4}\cos 4\theta) \\
&\quad + \rho^4 \cdot (-\frac{1}{16} - \frac{1}{32}\cos 2\theta + \frac{1}{16}\cos 4\theta + \frac{1}{32}\cos 6\theta).
\end{aligned}
$$

Therefore,

$$(18) \qquad \qquad f(\theta) = \frac{\psi(\theta)}{\kappa(\theta)}.$$

Integral

$$(19) \qquad \qquad \frac{1}{2\pi} \cdot \int_0^{2\pi} f(\theta)d\theta = 1,$$

is calculated by Maple® exactly.

For its calculation by the FFT-method,we:

- Discretize interval $[0, 2\pi]$ into $N = 2^n$ intervals, where $n > 3$ is positive integer,
- Calculate function in $k = 0, 1, 2, \ldots, N-1$ points, $\theta_k = \frac{2\pi}{N} \cdot k$, to obtain $f_k = f(\theta_k)$ values,
- Calculate FFT (the built-in operation in MathCad®) to obtain factor

$$a_0 = \frac{1}{2\pi} \cdot \int_0^{2\pi} f(\theta)d\theta, \text{ and}$$

- Round off the obtained a_0 to the nearest integer value.

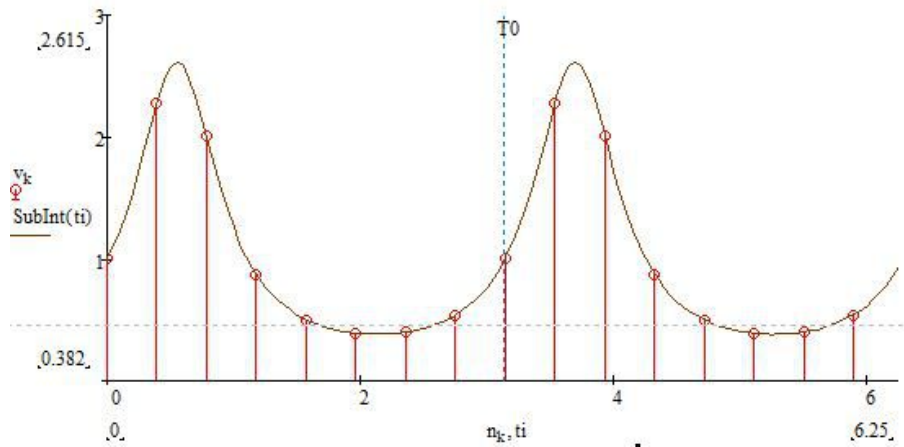Example of discretization of function $f(\theta)$ for $N = 2^4 = 16$ intervals is shown in Figure (2).

Figure 2. *Discretization of function for* $n = 4$

Values of a_0-factor for $\rho = 0.05$ differentiation values of n is shown in Table (1).

n	a_0(FFT)	$\log|a_0(FFT) - 1|$	Round $(a_0(FFT))$
4	0.99731	-2.570	1
5	1.00000	-5.651	1
6	1.00000	-11.118	1
7	1.00000	-15.353	1

Table 1. *Values of a_0 factor for $n > 3$*

As we see, it is necessary to have $N = 2^4$ points of discretization in this case to achieve the value of the index of the stationary point. When selecting number of points for the integrand discretization, it is necessary to keep in mind that the spectrum of the functions contains main cosine and sine harmonics so that higher harmonics in the spectrum have relatively small amplitude. Otherwise value of the index can be substantially deteriorated by the aliasing effect. This effect is illustrated in the next section.

4. VECTOR FIELD AND INDICES OF STATIONARY POINTS OF HOLLING-TANNER SYSTEM

In the Holling-Tanner system of equation, we assume that

$$(20) \qquad X = X(x,y) = b_1 x - b_2 x^2 - b_3 \frac{xy}{b_4 + x},$$

$$(21) \qquad Y = Y(x,y) = b_5 y - b_6 \frac{y^2}{x}.$$

Assuming that only non-negative y and positive x are considered, we can find three stationary points from equations $X = Y = 0$;

$$(22) \qquad x_1 = \frac{b_1}{b_2}, y_1 = 0,$$

$$(23) \qquad x_2 = \frac{-b_3 b_5 + b_1 b_6 - b_2 b_4 b_6 + \sqrt{4 b_1 b_2 b_4 b_6^2 + (-b_3 b_5 + b_1 b_6 - b_2 b_4 b_6)^2}}{2 b_2 b_6},$$

$$(24) \qquad y_2 = \frac{\frac{b_1 b_5}{b_2} - b_4 b_5 - \frac{b_3 b_5^2}{b_2 b_6} + \frac{b_5 \sqrt{4 b_1 b_2 b_4 b_6^2 + (-b_3 b_5 + b_1 b_6 - b_2 b_4 b_6)^2}}{b_2 b_6}}{2 b_6},$$

$$(25) \qquad x_3 = \frac{-b_3 b_5 + b_1 b_6 - b_2 b_4 b_6 - \sqrt{4 b_1 b_2 b_4 b_6^2 + (-b_3 b_5 + b_1 b_6 - b_2 b_4 b_6)^2}}{2 b_2 b_6},$$

$$(26) \qquad y_3 = \frac{\frac{b_1 b_5}{b_2} - b_4 b_5 - \frac{b_3 b_5^2}{b_2 b_6} - \frac{b_5 \sqrt{4 b_1 b_2 b_4 b_6^2 + (-b_3 b_5 + b_1 b_6 - b_2 b_4 b_6)^2}}{b_2 b_6}}{2 b_6}.$$

In these cases, $x_{1,2,3} > 0$ and $y_{1,2,3} \geq 0$, if $b_1.b_2, b_3, b_5, b_6$ are positive and $b_4 < 0$. At particular values of the b-coefficients $b_1 = 1, b_2 = 0.1, b_3 = 1, b_4 = -0.1, b_5 = 1, b_6 = 1.5$.

The corresponding roots are

$$x_1 = 10, \quad y_1 = 0, \tag{27}$$

$$x_2 \cong 0.32134, \quad y_2 \cong 0.21422, \tag{28}$$

$$x_3 \cong 3.11200, \quad y_3 \cong 2.07466. \tag{29}$$

At Equation (27), $x_1 = 10, y_1 = 0$, the linearized Holling-Tanner system in the vicinity of x_1, y_1 is

$$\Delta \dot{x}_1 \cong -\Delta x_1 - 1.01010 \cdot \Delta y_1, \tag{30}$$

$$\Delta \dot{y}_1 \cong \Delta y_1. \tag{31}$$

Eigenvalues of the linearized system of Equation (31) are

$$\lambda_{1,2} = \pm 1, \tag{32}$$

and hence, the stationary point is **saddle**.

At Equation (28), $x_2 = 0.32134, y_2 = 0.21422$, the linearized Holling-Tanner system in the vicinity of x_2, y_2 is

$$\Delta \dot{x}_2 \cong 1.37301 \cdot \Delta x_2 - 1.45180 \cdot \Delta y_2,$$

$$\Delta \dot{y}_2 \cong 0.66667 \cdot \Delta x_2 - \Delta y_2, \tag{33}$$

with corresponding eigenvalues

$$\lambda_1 \approx 0.84978; \lambda_2 = -0.47677, \tag{34}$$

hence, the stationary point is **saddle**.

In the third case Equation (29) at $x_3 \approx 3.11200, y_3 \cong 2.07466$, the linearized Holling-Tanner system in the vicinity of x_3, y_3 is

$$\Delta \dot{x}_3 \cong 0.40097 \Delta x_3 - 1.03320 \Delta y_2,$$

$$\Delta \dot{y}_3 \cong 0.66667 \Delta x_3 - \Delta y_3, \tag{35}$$

with corresponding eigenvalues

$$\lambda_{1,2} \approx -0.29977 \pm i0.44550. \tag{36}$$

and, the stationary point is **stable focus**.

The vector field of the Holling-Tanner system at the abovementioned parameters is shown in the $x - y$ plane $\ni (x \in [-1,12], y \in [-1,4])$ using that the *ListStreamPlot* built-in function of the Mathematica® in Figure (3).
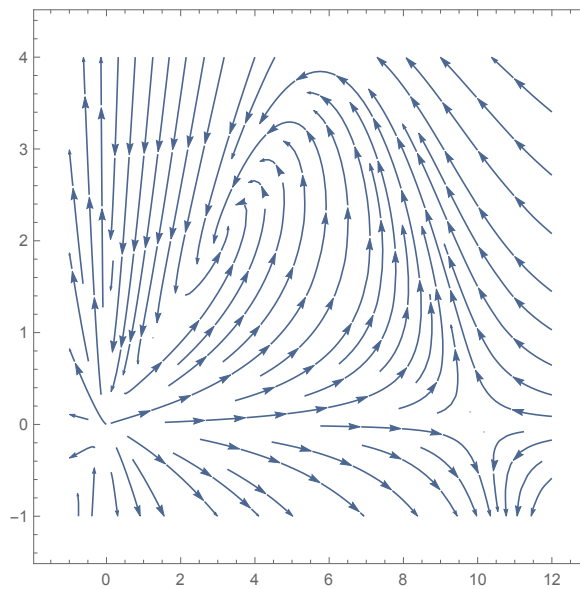

Figure 3. *Vector field of Holling-Tanner system*

To analyze the behaviour of the first stationary point $x_1 = 10, y_1 = 0$, we make change of variable.

$$x = 10 + x_1; y = y_1, \tag{37}$$

where $x_1 = \rho \cos \theta, y_1 = \rho \sin \theta$ and compose the Poincare integral with

$$\begin{cases} X_1(\theta) = 10 + \rho \cos \theta - \frac{(10 + \rho \cos \theta)^2}{10} - \frac{\rho \sin \theta (10 + \rho \cos \theta)}{\frac{99}{100} + \rho \cos \theta}, \\ Y_1(\theta) = \rho \sin \theta - \frac{3\rho^2 \sin^2 \theta}{20 + 2\rho \cos \theta}. \end{cases} \tag{38}$$

The results of discretization of the integrand

$$f_1 \rho(\theta) = \frac{X_1(\theta) \cdot \frac{dY_1(\theta)}{d\theta} - \frac{dX_1(\theta)}{d\theta} \cdot Y_1(\theta)}{X_1^2(\theta) + Y_1^2(\theta)}, \tag{39}$$

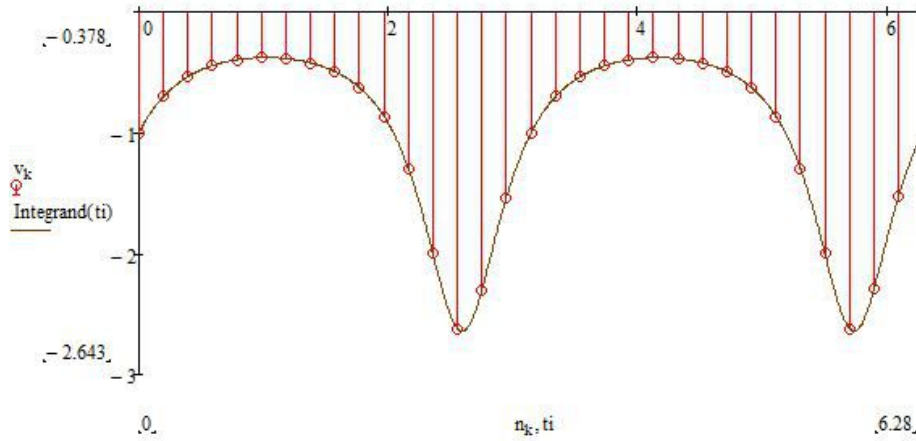in $N = 2^5$ points with $\rho = \frac{1}{100}$ are shown in Figure (4).

Figure 4. *Discretization of the integrand for $n = 5$*

Results of the FFT of the discretized function $v_k = f_1(\theta_k)$, where $\theta_k = \frac{2\pi}{k} \cdot k$, $k = 1, 2, \ldots, N-1$ and $N = 2^n$ are represented in Table (2).

n	a_0(FFT)	$\log|a_0(FFT)+1|$	Round $(a_0(FFT))$
3	0.97287	-1.567	-1
4	0.99719	-2.551	-1
5	-1.00000	-5.675	-1
6	-1.00000	-10.909	-1
7	-1.00000	-12.889	-1

Table 2. *Discretized Integrand of FFT for different values of n*

As we see the index of the stationary point $x_1 = 10, y_1 = 0$ equals to -1, which corresponds to

the saddle, can be obtained with minimum possible points of discretization.

Let us analyze the second stationary point $x_2 \cong 0.32134, y_2 \cong 0.21422$.

In this case,

$$X_2(\theta) \cong 0.32134 + \rho \cos \theta - 0.1(\rho \cos \theta + 0.32134)^2 - \frac{(0.32134 + \rho \cos \theta)(0.21422 + \rho \sin \theta)}{0.22134 + \rho \cos \theta},$$

(40)

$$Y_2(\theta) \cong 0.21422 + \rho \sin \theta - \frac{3(0.214222 + \rho \sin \theta)^2}{0.64267 + 2\rho \cos \theta}.$$

Discretization of the integrand

(41)
$$f_2\rho(\theta) = \frac{X_2(\theta) \cdot \frac{dY_2(\theta)}{d\theta} - \frac{dX_2(\theta)}{d\theta} \cdot Y_2(\theta)}{X_2^2(\theta) + Y_2^2(\theta)},$$

in $N = 2^6$ points with $\rho = \frac{1}{100}$ are shown in Figure (5).
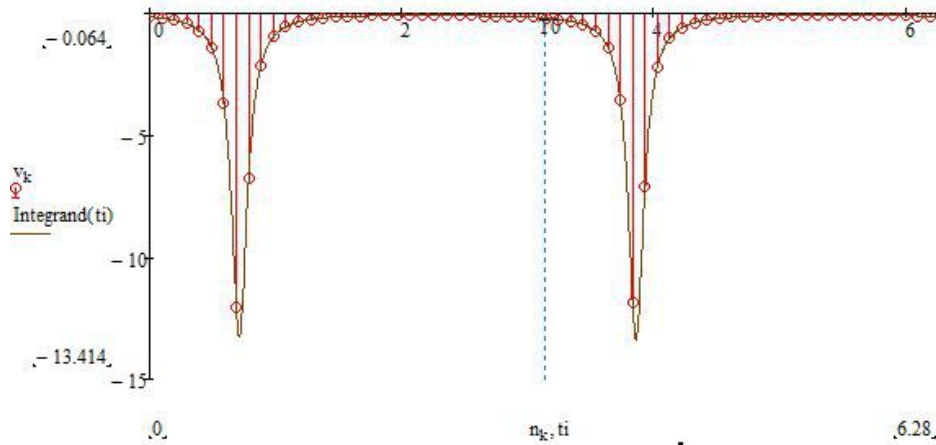

Figure 5. *Discretization of the integrand for* $n = 6$

Results of the FFT of the discretized integrand on $v_k = f_1(\theta_k)$, where $\theta_k = \frac{2\pi}{k} \cdot k$, $k = 1, 2, \ldots, N-1$ and $N = 2^n$ are given in Table (3).

n	a_0(FFT)	$\log|a_0(FFT)+1|$	Round $(a_0(FFT))$
4	-0.02600	-0.011	0
5	-0.43861	-0.251	0
6	-0.99874	-2.901	-1
7	-0.99987	-3.889	-1
8	-1.00000	-8.100	-1

Table 3. *Discretized Integrand of FFT for different values of n*

As we see the results of rounding of coefficient a_0(FFT) for $n = 4$ and $n = 5$ gives incorrect value of the index. For $n \geq 6$, we obtain satisfactory results. In this case, the index of the stationary point (x_2, y_2) is equal to -1, which correspond to the ***saddle***.

This is explained by the fact that the negative spikes in Figure (5) are sharp and hence, the spectrum of the Fourier transform contains substantial number of harmonics. Hence the incorrect results of the index calculation for $n = 4$ and $n = 5$ are explained by aliasing effect due to ignoring of higher frequency components in the Fourier spectrum of the integrand.

In the of third stationary points $x_3 \cong 3.11200, y_3 \cong 2.07466$, the components of the Poincare integral are

$$X_3(\theta) \cong 3.11200 + \rho \cos \theta - 0.1(3.11200 + \rho \cos \theta)^2 - \frac{(\rho \cos \theta + 3.11200)(\rho \sin \theta + 2.07466)}{3.11200 + \rho \cos \theta},$$

(42)

$$Y_3(\theta) \cong 2.07466 + \rho \sin \theta + \frac{3(2.07466 + \rho \sin \theta)^2}{6.22399 + 2\rho \cos \theta}.$$

Discretizing the Poincare integrand

(43)
$$f_3(\theta) = \frac{X_3(\theta) \cdot \frac{dY_3(\theta)}{d\theta} - \frac{dX_3(\theta)}{d\theta} \cdot Y_3(\theta)}{X_3^2(\theta) + Y_3^2(\theta)},$$
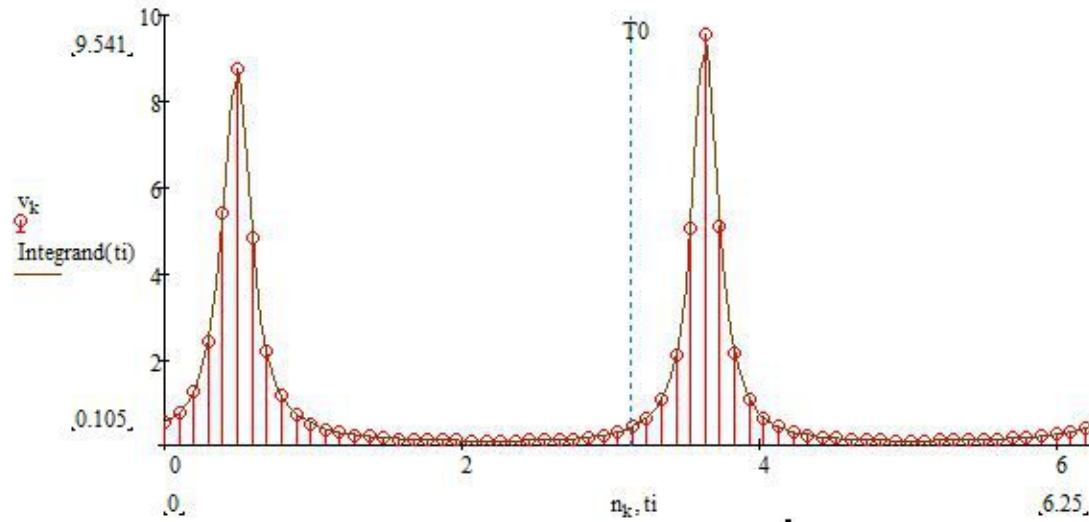
in $N = 2^6$ points , we obtain graph shown in Figure (6).

Figure 6. *Discretization of the integrand for n = 6*

Results of the corresponding FFTs for the different and $N = 2^n$ are given in Table (4).

n	a_0(FFT)	$\log|a_0(FFT) - 1|$	Round $(a_0(FFT))$
4	0.48025	-0.284	0
5	0.47048	-0.276	0
6	1.00182	-2.740	1
7	1.00000	-5.752	1
8	1.00000	-11.657	1

Table 4. *Discretized integrand of FFT for different values of n*

The results of incorrect calculation of the index of stationary points (x_3, y_3) is explained by the sharp positive spikes in the graph of the integrand and hence, the aliasing effect due to insufficient number of harmonics taken into consideration in the spectrum of the integrand. As we can see, the index of the stationary point (x_3, y_3) is equal to 1.

5. CONCLUSION

In this Chapter, two systems of equations (Van der Pol and Holling-Tanner) were investigated numerically and graphically. A novel algorithm (FFT-method) was proposed to numerically calculate the index of stationary points of the vector field by discretizing the function into interval, divided by N equal-distance of sub-intervals. The vector fields of the systems (Van der Pol and Holling-Tanner) were built using Mathematica®. The first term of the Fourier series expansion of the Poincare integrand is equal to the Poincare integral, hence the value of the index was numerically (approximately) calculated using the proposed FFT. The corresponding DFT were performed by using FFT, Figure (2, 4, 5 & 6), which is executed by the built-in functions in MathCad®. The stationary points were obtained as indicated in Equation (11) and Equation (27, 28 & 29), linearized in the vicinity of the corresponding roots, we obtain a stable focus for the Van der Pol equation, two stationary points were saddle and one stable focus for Holling-Tanner model. The Poincare integrands were calculated for all stationary points of the Van der Pol and Holling-Tanner systems and discretized in $N = 2^n$ points, where n is non-negative integer. After rounding off of the calculated approximate values of the indices, real values were obtained (see Tables (1, 2, 3 & 4)). It was shown that in accordance with the theory index of saddle points was equal to -1 and indices of the stable and unstable focus were equal to 1.

ACKNOWLEDGEMENT

CONFLICT OF INTERESTS

The author(s) declare that there is no conflict of interests.

REFERENCES

[1] S. Dragomir, I. Fedotov, On numerical evaluation of the winding number of a plane vector field, Bull. Math. Soc. Sci. Math. Roum. Nouv. Ser. 46(94) (2003), 61-70.

[2] G. Strang, Wavelets, Amer. Scientist, 82 (1994), 250–255.

[3] R.N. Bracewell, The Fourier transform, Sci. Amer. 260(6) (1989), 86–95.

[4] J. M.T. Heideman, D.H. Johnson, C.S. Burrus, Gauss and the history of the fast Fourier transform, Arch. History Exact Sci. 34 (3) (1985), 265–277.

[5] L. Zhong, L. Lichun, L. Huiqi, Application research on sparse fast Fourier transform algorithm in white Gaussian noise, Procedia Computer Sci. 107 (2017), 802–807.

[6] J.W. Cooley, J.W. Tukey, An algorithm for the machine calculation of complex Fourier series, Math. Comp. 19 (1965), 297–297.